# Porosity and Permeability Effects on the Seismo-Electric Reflection

A. Ranada Shaw, A.I.M. Denneman, and C.P.A. Wapenaar

Centre for Technical Geoscience, Delft University of Technology
P.O. Box 5028, 2600 GA Delft, The Netherlands

September 22, 2000

## 1 Introduction

The seismo-electric method is an integrated surveying technique for the shallow subsurface of the Earth, in which seismic sources and electromagnetic receivers are used. Although the existence of the seismo-electric conversion is known since the early 1930s [see the review paper of Beamish and Peart (1998)], the development of the seismo-electric method has been greatly enhanced since the publication of the experimental work of Thompson and Gist (1993) and the theoretical work of Pride and Haartsen (Pride, 1994; Pride and Haartsen, 1996; Haartsen and Pride, 1997). The recently obtained experimental results for the shallow subsurface of the Earth are very promising (Millar, 1995; Butler et al., 1996; Mikhailov et al., 1997; Russell et al., 1997; Zhu et al., 1999; Beamish, 1999; Garambois and Dietrich, 2000). In all these papers it is shown that the seismo-electric method is a useful tool to characterize parameters like fluid content and fluid geochemistry in the porous Earth's subsurface; hence, possible applications include groundwater detection and the detection of pollutant migration.

In measurements two distinct seismo-electric effects are observed: (i) the electromagnetic fields that accompany the body and surface waves during their propagation (it exists only in the area disturbed by the seismic wave and its apparent velocity is that of a seismic wave) and (ii) the independently propagating electromagnetic waves generated by seismic waves at interfaces where there is a contrast in the mechanical and/or electric parameters. In this paper we do not consider the first seismo-electric effect. Instead, we present all the necessary equations to calculate the reflection and transmission coefficients (in total 48 coefficients) belonging to an interface between two porous materials. At the end of this paper we present some numerical results belonging to a seismo-electric reflection (incident fast P-wave and reflected electromagnetic wave) due to a permeability/porosity contrast or a contrast in ion concentration.

## 2 Electrokinetic coupling: complete set of seven equations

According to Pride (1994) the seismic and electromagnetic wave propagation in a homogeneous, isotropic porous medium is governed by a complete set of seven equations. This set is obtained by applying an averaging procedure and, in the frequency domain, the first two equations of this set are the electromagnetic field equations given by

$$\boldsymbol{\nabla} \times \mathbf{H} = j\omega\epsilon_0\epsilon_{\mathrm{r}}\mathbf{E} + \mathbf{J}, \qquad \boldsymbol{\nabla} \times \mathbf{E} = -j\omega\mu\mathbf{H}, \tag{1}$$

where $\mathbf{E}$ is the electric field, $\mathbf{H}$ the magnetic field, $\mathbf{J}$ the induced electric current density, $\epsilon_0$ the dielectric permittivity of free space, $\epsilon_{\mathrm{r}}$ the relative permittivity of the porous material, and $\mu$ the magnetic permeability (for most porous materials $\mu$ is equal to the magnetic permeability of free space). Note that $\epsilon_{\mathrm{r}} = \epsilon_{\mathrm{s}} + \frac{\phi}{\alpha_\infty}(\epsilon_{\mathrm{f}} - \epsilon_{\mathrm{s}})$, where $\phi$ is the porosity, $\alpha_\infty$ the tortuosity, $\epsilon_{\mathrm{f}}$ the dielectric constant of the pore fluid, and $\epsilon_{\mathrm{s}}$ the dielectric constant of the solid skeleton.

The next three equations are the mechanical field equations given by

$$\boldsymbol{\tau}^{\mathrm{B}} = (H - 2G)(\boldsymbol{\nabla} \cdot \mathbf{u}^{\mathrm{s}})\mathbf{I} + C(\boldsymbol{\nabla} \cdot \mathbf{w})\mathbf{I} + G\left[\boldsymbol{\nabla}\mathbf{u}^{\mathrm{s}} + (\boldsymbol{\nabla}\mathbf{u}^{\mathrm{s}})^{T}\right], \tag{2}$$

$$\boldsymbol{\nabla} \cdot \boldsymbol{\tau}^{\mathrm{B}} = -\omega^2 \left(\rho_{\mathrm{B}}\mathbf{u}^{\mathrm{s}} + \rho_{\mathrm{f}}\mathbf{w}\right), \qquad -P = C\boldsymbol{\nabla} \cdot \mathbf{u}^{\mathrm{s}} + M\boldsymbol{\nabla} \cdot \mathbf{w}, \tag{3}$$

where $\boldsymbol{\tau}^{\mathrm{B}}$ is the bulk stress tensor, $P$ the pore fluid pressure, and $\mathbf{I}$ the unit tensor. The density $\rho_{\mathrm{B}} = \phi\rho_{\mathrm{f}} + (1-\phi)\rho_{\mathrm{s}}$ is the bulk density, in which $\rho_{\mathrm{f}}$ and $\rho_{\mathrm{s}}$ are the densities of the pore fluid and solid skeleton, respectively. The velocity $\dot{\mathbf{w}} = j\omega\mathbf{w} = j\omega\phi(\mathbf{u}^{\mathrm{f}} - \mathbf{u}^{\mathrm{s}})$ is the filtration velocity, where $\mathbf{u}^{\mathrm{f}}$ and $\mathbf{u}^{\mathrm{s}}$ are the wave displacements in the pore fluid and solid skeleton, respectively. We further note that $G$ is the shear modulus of the porous material, whereas the Biot moduli $H$, $C$, and $M$ are related to measurable quantities as (Biot, 1962; Haartsen and Pride, 1997)

$$H = \frac{K_{\mathrm{f}}(K_{\mathrm{s}} - K_{\mathrm{b}}) + \phi K_{\mathrm{b}}(K_{\mathrm{s}} - K_{\mathrm{f}})}{K_{\mathrm{f}}(1 - \phi - K_{\mathrm{b}}/K_{\mathrm{s}}) + \phi K_{\mathrm{s}}} + \frac{4}{3}G \tag{4}$$

$$C = \frac{K_{\mathrm{f}}(K_{\mathrm{s}} - K_{\mathrm{b}})}{K_{\mathrm{f}}(1 - \phi - K_{\mathrm{b}}/K_{\mathrm{s}}) + \phi K_{\mathrm{s}}}, \qquad M = \frac{K_{\mathrm{f}}K_{\mathrm{s}}}{K_{\mathrm{f}}(1 - \phi - K_{\mathrm{b}}/K_{\mathrm{s}}) + \phi K_{\mathrm{s}}}, \tag{5}$$

where $K_{\mathrm{s}}$ is the skeletal grain bulk modulus, $K_{\mathrm{f}}$ the pore fluid bulk modulus, and $K_{\mathrm{b}}$ the "jacketed" bulk modulus of the porous material [or dry frame bulk modulus as defined in Mavko et al. (1998)].

After having given the electromagnetic and mechanical field equations, we note that the coupling between the electromagnetic and mechanical wavefields is expressed by the following two transport equations (which are the last two equations of the complete set of seven equations):

$$\mathbf{J} = \sigma\mathbf{E} - \mathcal{L}\left(\boldsymbol{\nabla}P - \omega^2\rho_{\mathrm{f}}\mathbf{u}^{\mathrm{s}}\right), \qquad \dot{\mathbf{w}} = \mathcal{L}\mathbf{E} - \frac{k}{\eta}\left(\boldsymbol{\nabla}P - \omega^2\rho_{\mathrm{f}}\mathbf{u}^{\mathrm{s}}\right), \tag{6}$$

where $\sigma$ and $k$ are the electric conductivity and dynamical permeability of the porous material, respectively, and $\eta$ the shear viscosity of the pore fluid. Note that the electrokinetic coupling coefficient $\mathcal{L}$ determines the degree of coupling between the seismic and electromagnetic wave displacements.

According to Johnson et al. (1987) the dynamic permeability $k$ is given by

$$k = k_0\left[j\frac{\omega}{\omega_{\mathrm{c}}} + \sqrt{1 + j\frac{\mathcal{M}}{2}\frac{\omega}{\omega_{\mathrm{c}}}}\right]^{-1} \quad \text{with} \quad \omega_{\mathrm{c}} = \frac{\phi\eta}{k_0\rho_{\mathrm{f}}\alpha_\infty}, \tag{7}$$

where $k_0$ is the steady-state permeability, $\mathcal{M} \approx 1$ the so-called similarity parameter, $\omega$ the angular frequency, and $\omega_{\mathrm{c}}$ the roll-over frequency. Recently, Pride (1994) has derived rather complicated expressions for the frequency-dependent parameters $\sigma$ and $\mathcal{L}$; however, our numerical calculations show that many terms in these expressions have negligible influence on the relevant results. Of course, in our numerical code we continue using the full expressions for $\sigma$ and $\mathcal{L}$ as derived by Pride (1994), but we note that there will be a negligible change in the numerically obtained results if one would use the following simplified expressions:

$$\sigma = \frac{\phi\sigma_{\mathrm{f}}}{\alpha_\infty}, \qquad \mathcal{L} = \frac{-\phi\epsilon_0\epsilon_{\mathrm{f}}\zeta}{\alpha_\infty\eta}\left[1 + j\frac{2}{\mathcal{M}}\frac{\omega}{\omega_{\mathrm{c}}}\right]^{-1/2}, \tag{8}$$

where $\sigma_{\mathrm{f}}$ is the pore fluid conductivity and $\zeta$ the so-called zeta-potential (the potential drop across the outer Helmholtz double layer at the interface between the solid skeleton and the pore fluid). The pore fluid conductivity is related to the bulk ion concentrations $n_a$ as

$$\sigma_{\mathrm{f}} = \sum_a n_a b_a |q_a|, \tag{9}$$

where $q_a$ is the ion charge and the positive parameter $b_a$ the ion mobility (ion drift velocity per unit electric field). An analytical expression for the zeta-potential $\zeta$ has recently been derived by Revil et al. (1999) and this expression is consistent with the empirical relation for NaCl/quartz and KCl/quartz as obtained by Pride and Morgan (1991), i.e, with salinity $C = n_{\mathrm{Na}} = n_{\mathrm{Cl}}$ or $C = n_{\mathrm{K}} = n_{\mathrm{Cl}}$ this empirical relation is given by $\zeta(\text{in mV}) = 8 + 26 \log_{10} C(\text{in mol/liter})$.

## 3 Two independent sets of partial differential equations

At this point we restrict ourselves to a medium consisting of horizontal porous layers in which the waves propagate only in the $x$-$z$ plane (with the positive $z$-axis directed downwards). It is therefore convenient to apply to the complete set of seven equations [shown in Eqs. (1)–(3) and (6)] a Radon transform along the $x$-axis. Consequently, the derivatives with respect to $x$ in these equations are replaced by $-j\omega p$ (with horizontal slowness $p$), whereas the derivatives with respect to $y$ vanish; hence, one obtains the following two independent sets of partial differential equations:

$$\frac{\partial}{\partial z}\mathbf{Q}_{\mathrm{H}} = j\omega \mathbf{A}_{\mathrm{H}} \mathbf{Q}_{\mathrm{H}} = j\omega \begin{bmatrix} \mathbf{0}_{2\times 2} & \mathbf{A}_{1,\,\mathrm{H}} \\ \mathbf{A}_{2,\,\mathrm{H}} & \mathbf{0}_{2\times 2} \end{bmatrix} \mathbf{Q}_{\mathrm{H}}, \tag{10}$$

$$\frac{\partial}{\partial z}\mathbf{Q}_{\mathrm{V}} = j\omega \mathbf{A}_{\mathrm{V}} \mathbf{Q}_{\mathrm{V}} = j\omega \begin{bmatrix} \mathbf{0}_{4\times 4} & \mathbf{A}_{1,\,\mathrm{V}} \\ \mathbf{A}_{2,\,\mathrm{V}} & \mathbf{0}_{4\times 4} \end{bmatrix} \mathbf{Q}_{\mathrm{V}}, \tag{11}$$

where the vectors $\mathbf{Q}_{\mathrm{H}} = \left[\tau^{\mathrm{B}}_{yz},\ H_x,\ E_y,\ \dot{u}^{\mathrm{s}}_y\right]^T$ and $\mathbf{Q}_{\mathrm{V}} = [\dot{u}^{\mathrm{s}}_z,\ \dot{w}_z,\ \tau^{\mathrm{B}}_{xz},\ H_y,\ E_x,\ \tau^{\mathrm{B}}_{zz},\ -P,\ \dot{u}^{\mathrm{s}}_x]^T$ (with velocities $\dot{\mathbf{u}}^{\mathrm{s}} = j\omega \mathbf{u}^{\mathrm{s}}$ and $\dot{\mathbf{w}} = j\omega \mathbf{w}$) contain the parameters that are continuous across the interfaces between the horizontal porous layers [i.e., we apply the open-pore boundary conditions of Deresiewicz and Skalak (1963)]. In addition, the matrices $\mathbf{0}_{2\times 2}$ and $\mathbf{0}_{4\times 4}$ are square matrices containing only zeros and the system matrices $\mathbf{A}_{1,\,\mathrm{H}}$, $\mathbf{A}_{2,\,\mathrm{H}}$, $\mathbf{A}_{1,\,\mathrm{V}}$, and $\mathbf{A}_{2,\,\mathrm{V}}$ are given by

$$\mathbf{A}_{1,\,\mathrm{H}} = \begin{bmatrix} \rho_{\mathrm{f}}\mathcal{L} & \rho_{\mathrm{B}} - \frac{\rho_{\mathrm{f}}^2}{\rho_{\mathrm{E}}} - p^2 G \\ \epsilon - \frac{p^2}{\mu} & -\rho_{\mathrm{f}}\mathcal{L} \end{bmatrix}, \qquad \mathbf{A}_{2,\,\mathrm{H}} = \begin{bmatrix} 0 & \mu \\ \frac{1}{G} & 0 \end{bmatrix}, \tag{12}$$

$$\mathbf{A}_{1,\,\mathrm{V}} = \begin{bmatrix} 0 & \frac{M}{\Delta} & \frac{-C}{\Delta} & p\left(1 - \frac{2GM}{\Delta}\right) \\ p\mathcal{L} & \frac{-C}{\Delta} & \frac{H}{\Delta} - \frac{p^2}{\rho_{\mathrm{E}}} & p\left(\frac{2GC}{\Delta} - \frac{\rho_{\mathrm{f}}}{\rho_{\mathrm{E}}}\right) \\ \rho_{\mathrm{f}}\mathcal{L} & p\left(1 - \frac{2GM}{\Delta}\right) & p\left(\frac{2GC}{\Delta} - \frac{\rho_{\mathrm{f}}}{\rho_{\mathrm{E}}}\right) & \rho_{\mathrm{B}} - \frac{\rho_{\mathrm{f}}^2}{\rho_{\mathrm{E}}} - 4p^2 G\left(1 - \frac{GM}{\Delta}\right) \\ -\epsilon & 0 & p\mathcal{L} & \rho_{\mathrm{f}}\mathcal{L} \end{bmatrix}, \tag{13}$$

$$\mathbf{A}_{2,\,\mathrm{V}} = \begin{bmatrix} 0 & \frac{p\mathcal{L}\rho_{\mathrm{E}}}{\epsilon - \rho_{\mathrm{E}}\mathcal{L}^2} & 0 & \frac{p^2}{\epsilon - \rho_{\mathrm{E}}\mathcal{L}^2} - \mu \\ \rho_{\mathrm{B}} & \rho_{\mathrm{f}} & p & 0 \\ \rho_{\mathrm{f}} & \frac{\epsilon\rho_{\mathrm{E}}}{\epsilon - \rho_{\mathrm{E}}\mathcal{L}^2} & 0 & \frac{p\mathcal{L}\rho_{\mathrm{E}}}{\epsilon - \rho_{\mathrm{E}}\mathcal{L}^2} \\ p & 0 & \frac{1}{G} & 0 \end{bmatrix}, \tag{14}$$

in which the parameters $\Delta$, $\rho_{\rm E}$, and $\epsilon$ are defined as

$$\Delta = HM - C^2, \qquad \rho_{\rm E} = \frac{\eta}{j\omega k}, \qquad \epsilon = \epsilon_0\epsilon_{\rm r} + \frac{\sigma}{j\omega}. \tag{15}$$

Note that Haartsen and Pride (1997) also obtained the two independent sets of differential equations given by Eqs. (10) and (11); however, since they use the vectors $\mathbf{Q}_{\rm H} = \left[u_y^{\rm s},\ \tau_{yz}^{\rm B},\ H_x,\ E_y\right]^T$ and $\mathbf{Q}_{\rm V} = [u_x^{\rm s},\ u_z^{\rm s},\ w_z,\ \tau_{xz}^{\rm B},\ \tau_{zz}^{\rm B},\ -P,\ H_y,\ E_x]^T$ instead of the ones given before, their expressions for the matrices $\mathbf{A}_{\rm H}$ and $\mathbf{A}_{\rm V}$ are more complicated than the ones given in this paper.

## 4 Coupling between SH-waves and TE-waves

When a horizontally polarized shear wave (SH-mode) propagates in the $x$-$z$ plane, its propagation is not coupled to the other three seismic wavefields (the fast and slow P-waves and the vertically polarized shear wave); however, the SH-wave generates electric currents in the $y$-direction and these currents couple to the electromagnetic wavefield with transverse electric polarization (TE-mode). As already shown by Haartsen and Pride (1997) this SHTE-coupling is represented by the set of differential equations given by Eq. (10). The system matrix $\mathbf{A}_{\rm H}$ in Eq. (10) can be used to determine the velocities of the SH-wave and TE-wave in a homogeneous porous layer by considering the case of a horizontally propagating wave with velocity $v = 1/p$. For this specific case the left hand side of Eq. (10) becomes zero (i.e., there is no $z$-dependency) and the non-trivial solution for the resulting linear set of equations is the one for which the determinant $|\mathbf{A}_{\rm H}| = |\mathbf{A}_{1,\,\rm H}|\,|\mathbf{A}_{2,\,\rm H}|$ vanishes. Consequently, since $|\mathbf{A}_{2,\,\rm H}| \neq 0$, one simply has to find a horizontal slowness $p = 1/v$ for which $|\mathbf{A}_{1,\,\rm H}|$ is zero, i.e., one finds (Pride and Haartsen, 1996)

$$\frac{2}{v^2} = \frac{\rho_{\rm B} - \rho_{\rm f}^2/\rho_{\rm E}}{G} + \epsilon\mu \pm \sqrt{\left(\frac{\rho_{\rm B} - \rho_{\rm f}^2/\rho_{\rm E}}{G} - \epsilon\mu\right)^2 - 4\frac{\mu\rho_{\rm f}^2\mathcal{L}^2}{G}}, \tag{16}$$

where the plus sign is associated with the velocity of the SH-wave (denoted by $v_{\rm s}$) and the minus sign with the velocity of the TE-wave (denoted by $v_{\rm em}$).

The wave field represented by vector $\mathbf{Q}_{\rm H}$ in Eq. (10) is decomposed (for arbitrary $p$) in downgoing and upgoing wavefields by using the transformation $\mathbf{Q}_{\rm H} = \mathbf{L}_{\rm H}\mathbf{D}_{\rm H}$, where matrix $\mathbf{L}_{\rm H}$ contains the eigenvectors of matrix $\mathbf{A}_{\rm H}$. By using the results of Pride and Haartsen (1996), we find that matrix $\mathbf{L}_{\rm H}$ is given by $\mathbf{L}_{\rm H} = j\omega\left[\mathbf{a}_{\rm s}^+,\ \mathbf{a}_{\rm em}^+,\ \mathbf{a}_{\rm s}^-,\ \mathbf{a}_{\rm em}^-\right]$, in which

$$\mathbf{a}_n^{\pm} = \begin{bmatrix} \mp q_n G \\ \pm q_n \gamma_n \\ -\mu\gamma_n \\ 1 \end{bmatrix} \quad \text{with} \quad \gamma_n = \frac{\mathcal{L}\rho_{\rm E}(G - \rho_{\rm B}v_n^2)}{(\epsilon - \rho_{\rm E}\mathcal{L}^2)\mu\rho_{\rm f}v_n^2 - \rho_{\rm f}}, \quad \text{where} \quad n = \{\rm s,\ em\}. \tag{17}$$

Here, $q_n$ represents the two vertical slownesses belonging to the SH-wave and TE-wave [with $p^2 + q_n^2 = 1/v_n^2$ and $\mathrm{Im}(q_n) < 0$]. Note that $\pm q_n$ are the eigenvalues of $\mathbf{A}_{\rm H}$; hence, by combining Eq. (10) with the relation $\mathbf{L}_{\rm H}^{-1}\mathbf{A}_{\rm H}\mathbf{L}_{\rm H} = \mathrm{diag}[-q_{\rm s},\ -q_{\rm em},\ q_{\rm s},\ q_{\rm em}]$ one finds in a homogeneous porous layer

$$\mathbf{D}_{\rm H} = \begin{bmatrix} \mathbf{D}_{\rm H}^+ \\ \mathbf{D}_{\rm H}^- \end{bmatrix} \quad \text{with} \quad \mathbf{D}_{\rm H}^+ = \begin{bmatrix} d_{\rm sh}^+ \exp(-j\omega q_{\rm s} z) \\ d_{\rm te}^+ \exp(-j\omega q_{\rm em} z) \end{bmatrix} \quad \text{and} \quad \mathbf{D}_{\rm H}^- = \begin{bmatrix} d_{\rm sh}^- \exp(j\omega q_{\rm s} z) \\ d_{\rm te}^- \exp(j\omega q_{\rm em} z) \end{bmatrix}, \tag{18}$$

where $\mathbf{D}_{\rm H}^+$ and $\mathbf{D}_{\rm H}^-$ are the downgoing and the upgoing wavefield, respectively. Note that $d_{\rm sh}^+$, $d_{\rm te}^+$, $d_{\rm sh}^-$, and $d_{\rm te}^-$ are displacement amplitudes with dimension "meter".

## 5 Coupling between fast and slow P-waves, SV-waves, and TM-waves

When a fast P-wave, slow P-wave, or a vertically polarized shear wave (SV-mode) propagates in the $x$-$z$ plane, it generates electric currents in the $x$-$z$ plane and these currents couple to the electromagnetic wavefield with transverse magnetic polarization (TM-mode). This PSVTM-coupling is represented by the set of differential equations given by Eq. (11) (Haartsen and Pride, 1997). Similarly to the SHTE-case in the previous section, the system matrix $\mathbf{A}_{\mathrm{V}}$ in Eq. (11) can be used to determine the velocities of the fast and slow P-waves, SV-wave and TM-wave: find a horizontal slowness $p = 1/v$ for which $|\mathbf{A}_{1,\,\mathrm{V}}|\,|\mathbf{A}_{2,\,\mathrm{V}}| = 0$. As expected, the solution for $|\mathbf{A}_{2,\,\mathrm{V}}| = 0$ results in velocities for the SV-wave and TM-wave as given in Eq. (16), in which the plus and minus sign are associated with the SV-wave ($v_{\mathrm{s}}$) and TM-wave ($v_{\mathrm{em}}$), respectively. On the other hand, the solution for $|\mathbf{A}_{1,\,\mathrm{V}}| = 0$ results in (Pride and Haartsen, 1996)

$$\frac{2}{v^2} = \nu \pm \sqrt{\nu^2 - \frac{4}{\Delta}\left(\frac{\epsilon\rho_{\mathrm{E}}\rho_{\mathrm{B}}}{\epsilon - \rho_{\mathrm{E}}\mathcal{L}^2} - \rho_{\mathrm{f}}^2\right)} \quad \text{with} \quad \nu = \rho_{\mathrm{B}}\frac{M}{\Delta} + \frac{\epsilon\rho_{\mathrm{E}}}{\epsilon - \rho_{\mathrm{E}}\mathcal{L}^2}\frac{H}{\Delta} - 2\rho_{\mathrm{f}}\frac{C}{\Delta}, \tag{19}$$

where the smallest $|v|$ (in most cases associated with the plus sign) is the velocity of the slow P-wave (denoted by $v_{\mathrm{ps}}$) and the largest one is the velocity of the fast P-wave (denoted by $v_{\mathrm{pf}}$).

Similarly to the SHTE-case in the previous section, the vector $\mathbf{Q}_{\mathrm{V}}$ in Eq. (11) is transformed as $\mathbf{Q}_{\mathrm{V}} = \mathbf{L}_{\mathrm{V}}\mathbf{D}_{\mathrm{V}}$, where matrix $\mathbf{L}_{\mathrm{V}}$ contains the eigenvectors of matrix $\mathbf{A}_{\mathrm{V}}$. By using the results of Pride and Haartsen (1996), we find that $\mathbf{L}_{\mathrm{V}} = j\omega\left[\mathbf{b}_{\mathrm{pf}}^{+},\ \mathbf{b}_{\mathrm{ps}}^{+},\ \mathbf{b}_{\mathrm{s}}^{+},\ \mathbf{b}_{\mathrm{em}}^{+},\ \mathbf{b}_{\mathrm{pf}}^{-},\ \mathbf{b}_{\mathrm{ps}}^{-},\ \mathbf{b}_{\mathrm{s}}^{-},\ \mathbf{b}_{\mathrm{em}}^{-}\right]$, in which

$$\mathbf{b}_m^{\pm} = \begin{bmatrix} \pm q_m v_m \\ \pm q_m v_m \gamma_m \\ \mp 2p q_m v_m G \\ 0 \\ -(p v_m \gamma_m \rho_{\mathrm{E}}\mathcal{L})/(\epsilon - \rho_{\mathrm{E}}\mathcal{L}^2) \\ (2Gp^2 v_m^2 - H - \gamma_m C)/v_m \\ -(C + \gamma_m M)/v_m \\ p v_m \end{bmatrix}, \qquad \mathbf{b}_n^{\pm} = \begin{bmatrix} \pm p v_n \\ \pm p(G - \rho_{\mathrm{B}}v_n^2)/(v_n\rho_{\mathrm{f}}) \\ \pm v_n(q_n^2 - p^2)G \\ \pm \gamma_n/v_n \\ \mu q_n v_n \gamma_n \\ -2p q_n v_n G \\ 0 \\ -q_n v_n \end{bmatrix}, \tag{20}$$

where $\gamma_n$ is defined in Eq. (17), whereas $\gamma_m$ is defined as

$$\gamma_m = \frac{H - \rho_{\mathrm{B}}v_m^2}{\rho_{\mathrm{f}}v_m^2 - C} \qquad \text{with} \qquad m = \{\mathrm{pf},\,\mathrm{ps}\}. \tag{21}$$

Here, $q_n$ and $q_m$ represent the four vertical slownesses belonging to the SV-wave, TM-wave, fast P-wave and slow P-wave [$p^2 + q_n^2 = 1/v_n^2$ and $\mathrm{Im}(q_n) < 0$; $p^2 + q_m^2 = 1/v_m^2$ and $\mathrm{Im}(q_m) > 0$]. Note that $\pm q_n$ and $\pm q_m$ are the eigenvalues of $\mathbf{A}_{\mathrm{V}}$; hence, by combining Eq. (11) with the relation $\mathbf{L}_{\mathrm{V}}^{-1}\mathbf{A}_{\mathrm{V}}\mathbf{L}_{\mathrm{V}} = \mathrm{diag}[-q_{\mathrm{pf}},\ -q_{\mathrm{ps}},\ -q_{\mathrm{s}},\ -q_{\mathrm{em}},\ q_{\mathrm{pf}},\ q_{\mathrm{ps}},\ q_{\mathrm{s}},\ q_{\mathrm{em}}]$ one finds in a homogeneous porous layer

$$\mathbf{D}_{\mathrm{V}} = \begin{bmatrix} \mathbf{D}_{\mathrm{V}}^{+} \\ \mathbf{D}_{\mathrm{V}}^{-} \end{bmatrix} \quad \text{with} \quad \mathbf{D}_{\mathrm{V}}^{+} = \begin{bmatrix} d_{\mathrm{pf}}^{+}\exp(-j\omega q_{\mathrm{pf}} z) \\ d_{\mathrm{ps}}^{+}\exp(-j\omega q_{\mathrm{ps}} z) \\ d_{\mathrm{sv}}^{+}\exp(-j\omega q_{\mathrm{s}} z) \\ d_{\mathrm{tm}}^{+}\exp(-j\omega q_{\mathrm{em}} z) \end{bmatrix} \quad \text{and} \quad \mathbf{D}_{\mathrm{V}}^{-} = \begin{bmatrix} d_{\mathrm{pf}}^{-}\exp(j\omega q_{\mathrm{pf}} z) \\ d_{\mathrm{ps}}^{-}\exp(j\omega q_{\mathrm{ps}} z) \\ d_{\mathrm{sv}}^{-}\exp(j\omega q_{\mathrm{s}} z) \\ d_{\mathrm{tm}}^{-}\exp(j\omega q_{\mathrm{em}} z) \end{bmatrix}. \tag{22}$$

Again, the parameters $d_{\mathrm{pf}}^{+}, \ldots, d_{\mathrm{tm}}^{-}$ in the downgoing and upgoing wavefields ($\mathbf{D}_{\mathrm{V}}^{+}$ and $\mathbf{D}_{\mathrm{V}}^{-}$) are displacement amplitudes with dimension "meter".

## 6 Reflection and transmission coefficients

The results obtained so far are used to calculate the reflection and transmission coefficients belonging to an interface (at depth $z=0$) between two porous half-spaces. The vectors $\mathbf{Q}_{\mathrm{H}}=\mathbf{L}_{\mathrm{H}}\mathbf{D}_{\mathrm{H}}$ and $\mathbf{Q}_{\mathrm{V}}=\mathbf{L}_{\mathrm{V}}\mathbf{D}_{\mathrm{V}}$ are continuous across this interface, so one obtains

$$\mathbf{L}_{\mathrm{H,\,U}}\begin{bmatrix}\mathbf{D}^{+}_{\mathrm{H,\,U}}\\ \mathbf{D}^{-}_{\mathrm{H,\,U}}\end{bmatrix}=\mathbf{L}_{\mathrm{H,\,L}}\begin{bmatrix}\mathbf{D}^{+}_{\mathrm{H,\,L}}\\ \mathbf{0}_{2\times1}\end{bmatrix},\qquad \mathbf{L}_{\mathrm{V,\,U}}\begin{bmatrix}\mathbf{D}^{+}_{\mathrm{V,\,U}}\\ \mathbf{D}^{-}_{\mathrm{V,\,U}}\end{bmatrix}=\mathbf{L}_{\mathrm{V,\,L}}\begin{bmatrix}\mathbf{D}^{+}_{\mathrm{V,\,L}}\\ \mathbf{0}_{4\times1}\end{bmatrix},\tag{23}$$

where $\mathbf{0}_{2\times1}$ and $\mathbf{0}_{4\times1}$ are vectors containing only zeros and the subscripts U and L refer to the upper and lower half-space, respectively. We further note that (i) the incident wavefield ($\mathbf{D}^{+}_{\mathrm{H,\,U}}$ and $\mathbf{D}^{+}_{\mathrm{V,\,U}}$) is a downgoing one in the upper half-space, (ii) the reflected wavefield ($\mathbf{D}^{-}_{\mathrm{H,\,U}}$ and $\mathbf{D}^{-}_{\mathrm{V,\,U}}$) is an upgoing one in the upper half-space, (iii) the transmitted wavefield ($\mathbf{D}^{+}_{\mathrm{H,\,L}}$ and $\mathbf{D}^{+}_{\mathrm{V,\,L}}$) is a downgoing one in the lower half-space, and (iv) the upgoing wavefield in the lower half-space ($\mathbf{D}^{-}_{\mathrm{H,\,L}}$ and $\mathbf{D}^{-}_{\mathrm{V,\,L}}$) is set to zero. Consequently, the reflection and transmission matrices $\mathbf{R}_{\mathrm{H}}$, $\mathbf{T}_{\mathrm{H}}$, $\mathbf{R}_{\mathrm{V}}$, and $\mathbf{T}_{\mathrm{V}}$ are related to the incident and reflected or transmitted wavefields as

$$\mathbf{D}^{-}_{\mathrm{H,\,U}}=\mathbf{R}_{\mathrm{H}}\mathbf{D}^{+}_{\mathrm{H,\,U}},\qquad \mathbf{D}^{+}_{\mathrm{H,\,L}}=\mathbf{T}_{\mathrm{H}}\mathbf{D}^{+}_{\mathrm{H,\,U}},\tag{24}$$

$$\mathbf{D}^{-}_{\mathrm{V,\,U}}=\mathbf{R}_{\mathrm{V}}\mathbf{D}^{+}_{\mathrm{V,\,U}},\qquad \mathbf{D}^{+}_{\mathrm{V,\,L}}=\mathbf{T}_{\mathrm{V}}\mathbf{D}^{+}_{\mathrm{V,\,U}}.\tag{25}$$

By combining Eqs. (23), (24), and (25) in an appropriate way we obtain

$$\begin{bmatrix}\mathbf{T}_{\mathrm{H}}^{-1}\\ \mathbf{R}_{\mathrm{H}}\mathbf{T}_{\mathrm{H}}^{-1}\end{bmatrix}=\mathbf{L}^{-1}_{\mathrm{H,\,U}}\mathbf{L}_{\mathrm{H,\,L}}\begin{bmatrix}\mathbf{I}_{2\times2}\\ \mathbf{0}_{2\times2}\end{bmatrix},\tag{26}$$

$$\begin{bmatrix}\mathbf{T}_{\mathrm{V}}^{-1}\\ \mathbf{R}_{\mathrm{V}}\mathbf{T}_{\mathrm{V}}^{-1}\end{bmatrix}=\mathbf{L}^{-1}_{\mathrm{V,\,U}}\mathbf{L}_{\mathrm{V,\,L}}\begin{bmatrix}\mathbf{I}_{4\times4}\\ \mathbf{0}_{4\times4}\end{bmatrix},\tag{27}$$

where $\mathbf{I}_{2\times2}$ and $\mathbf{I}_{4\times4}$ are identity matrices. Note that the matrices $\mathbf{R}_{\mathrm{H}}$, $\mathbf{T}_{\mathrm{H}}$, $\mathbf{R}_{\mathrm{V}}$, and $\mathbf{T}_{\mathrm{V}}$ contain the reflection and transmission coefficients belonging to the interface between two porous half-spaces (in total 48 coefficients). For instance, the reflection matrix $\mathbf{R}_{\mathrm{V}}$ relates the incident wavefield with the reflected wavefield as

$$\underbrace{\begin{bmatrix}d^{-}_{\mathrm{pf}}\\ d^{-}_{\mathrm{ps}}\\ d^{-}_{\mathrm{sv}}\\ d^{-}_{\mathrm{tm}}\end{bmatrix}}_{\text{Reflected wavefield}}=\underbrace{\begin{bmatrix}R^{\mathrm{pf}}_{\mathrm{pf}} & R^{\mathrm{pf}}_{\mathrm{ps}} & R^{\mathrm{pf}}_{\mathrm{sv}} & R^{\mathrm{pf}}_{\mathrm{tm}}\\ R^{\mathrm{ps}}_{\mathrm{pf}} & R^{\mathrm{ps}}_{\mathrm{ps}} & R^{\mathrm{ps}}_{\mathrm{sv}} & R^{\mathrm{ps}}_{\mathrm{tm}}\\ R^{\mathrm{sv}}_{\mathrm{pf}} & R^{\mathrm{sv}}_{\mathrm{ps}} & R^{\mathrm{sv}}_{\mathrm{sv}} & R^{\mathrm{sv}}_{\mathrm{tm}}\\ R^{\mathrm{tm}}_{\mathrm{pf}} & R^{\mathrm{tm}}_{\mathrm{ps}} & R^{\mathrm{tm}}_{\mathrm{sv}} & R^{\mathrm{tm}}_{\mathrm{tm}}\end{bmatrix}}_{\text{Reflection coefficients}}\underbrace{\begin{bmatrix}d^{+}_{\mathrm{pf}}\\ d^{+}_{\mathrm{ps}}\\ d^{+}_{\mathrm{sv}}\\ d^{+}_{\mathrm{tm}}\end{bmatrix}}_{\text{Incident wavefield}}\tag{28}$$

where, e.g., the coefficient $R^{\mathrm{tm}}_{\mathrm{pf}}$ corresponds to an incident fast P-wave and a reflected TM-wave.

## 7 Permeability/porosity contrast and contrast in ion concentration

To illustrate the analytical results obtained so far, we now consider the reflection coefficient $R^{\mathrm{tm}}_{\mathrm{pf}}$ belonging to an interface between two nearly identical porous half-spaces, i.e., they differ only in (i) permeability and porosity or (ii) ion concentration in the pores. Both porous half-spaces are

characterized by $K_s = 40$ GPa, $K_b = 4$ GPa, $G = 3$ GPa, $\rho_s = 2700$ kgm$^{-3}$, $\epsilon_s = 4$, and $\alpha_\infty = 2$, and the pore fluids consist of $Na^+$ and $Cl^-$ ions dissolved in water ($K_f = 2.2$ GPa, $\rho_f = 1000$ kgm$^{-3}$, $\eta = 0.001$ Pas, $b_{Na} = 5.2\ 10^{-8}$ m$^2$s$^{-1}$V$^{-1}$, $b_{Cl} = 7.9\ 10^{-8}$ m$^2$s$^{-1}$V$^{-1}$, and $\epsilon_f = 80$). An incident fast P-wave is converted in a reflected TM-wave with propagation velocity $v_{em,\,U}$ due to a permeability/porosity contrast (see Fig. 1a) or an ion concentration contrast (see Fig. 1b). Note that in both porous half-spaces the permeability $k_0$ and porosity $\phi$ are related to each other as $k_0 \propto \phi^3$ [Kozeny-Carman relation (Mavko et al., 1998)].

By using Eqs. (27) and (28) the reflection coefficient $R^{tm}_{pf}$ is calculated as a function of the horizontal slowness $p$ times velocity $|v_{em,\,U}|$. The region $0 < p|v_{em,\,U}| < 1$ corresponds to reflection angles from zero to ninety degrees and for $p|v_{em,\,U}| \geq 1$ the reflected TM-wave becomes evanescent. Since $|v_{em,\,U}|$ is much larger than the incident fast P-wave velocity $|v_{pf,\,U}|$, the region $0 < p|v_{em,\,U}| < 1$ also corresponds to very small incident angles (much smaller than one degree); although exact normal incidence does not result in seismo-electric reflection, the non-evanescent reflected TM-waves come only into existence at very small deviations of this exact normal incidence. In many papers on seismo-electric reflection in near-surface experiments it is shown that contrasts as in Fig. 1 result in a measurable response (after some signal processing to improve the signal to noise ratio). The current availability of the reflection coefficient $R^{tm}_{pf}$ (and all the other coefficients) is especially useful to acquire more physical insight in the dependencies of the seismo-electric reflection on the many possible contrasts at interfaces between two porous materials.

## 8 Concluding remarks

The work presented in this paper can be seen as an extension of the theoretical work of Pride and Haartsen (Pride, 1994; Pride and Haartsen, 1996; Haartsen and Pride, 1997). Starting with Biot's equations coupled to Maxwell's equations we finally arrive at expressions given by Eqs. (26) and (27) that can be used to calculate the reflection and transmission coefficients belonging to an interface between two porous media. In our current research we are mainly interested in the seismo-

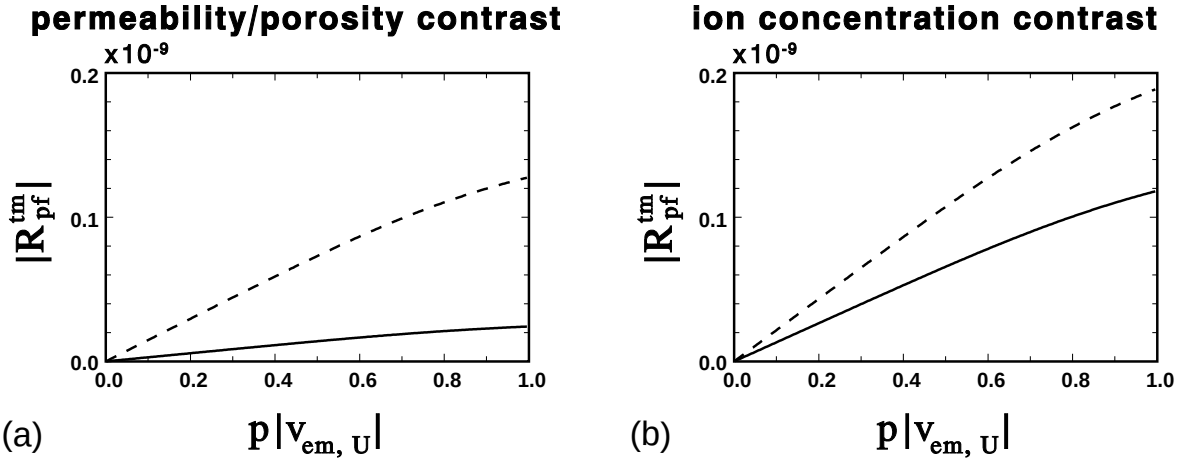


Figure 1: Incoming fast P-wave and reflected TM-wave with velocity $v_{em,\,U}$ ($f = \omega/2\pi = 100$ Hz): the reflection coefficient $R^{tm}_{pf}$ as a function of the horizontal slowness $p$ times velocity $|v_{em,\,U}|$. In upper porous half-space: salinity $C = n_{Na} = n_{Cl} = 10^{-6}$ mol/liter, porosity $\phi = 0.2$, and permeability $k_0 = 0.16$ Darcy. In lower porous half-space: (a) $\phi = 0.3$ and $k_0 = 0.54$ Darcy (solid line) and $\phi = 0.4$ and $k_0 = 1.28$ Darcy (dashed line) with $C = 10^{-6}$ mol/liter and (b) $C = 10^{-5}$ mol/liter (solid line) and $C = 10^{-4}$ mol/liter (dashed line) with $\phi = 0.2$ and $k_0 = 0.16$ Darcy.

electric reflection $R_{\rm pf}^{\rm tm}$: an incident fast P-wave converts into a reflected TM-wave. By using the analytical results presented in this paper it is now possible to acquire a good physical understanding of the dependencies of $R_{\rm pf}^{\rm tm}$ on the many possible contrasts at interfaces between porous materials. A lot of research still has to be done, but the results obtained by many researchers so far make clear that the seismo-electric method has the potential to image permeability/porosity contrasts and/or ion concentration contrasts in the shallow subsurface of the Earth.

**References**


Beamish, D., and Peart, R. J., 1998, Electrokinetic geophysics — a review: Terra Nova, **10**, 48–55.

Beamish, D., 1999, Characteristics of near-surface electrokinetic coupling: Geophys. J. Int., **137**, 231–242.

Biot, M. A., 1962, Mechanics of deformation and acoustic propagation in porous media: J. Appl. Phys., **33**, 1482–1498.

Butler, K. E., Russell, R. D., Kepic, A. W., and Maxwell, M., 1996, Measurement of the seismo-electric response from a shallow boundary: Geophysics, **61**, 1769–1778.

Deresiewicz, H., and Skalak, R., 1963, On uniqueness in dynamic poroelasticity: Bull. Seis. Soc. Am., **53**, 783–788.

Garambois, S., and Dietrich, M., 2000/2001, Seismo-eelectric wave conversions in porous media: Field measurements and transfer function analysis: accepted for publication in Geophysics.

Haartsen, M. W., and Pride, S. R., 1997, Electroseismic waves from point sources in layered media: J. Geophys. Res, **102**, 24745–24769.

Johnson, D. L., Koplik, J., and Dashen, R., 1987, Theory of dynamic permeability and tortuosity in fluid-saturated porous media: J. Fluid Mech., **176**, 379–402.

Mavko, G., Mukerji, T., and Dvorkin, J., 1998, The rock physics handbook: Tools for seismic analysis in porous media: Cambridge Univ. Press.

Mikhailov, O. V., Haartsen, M. W., and Toksöz, M. N., 1997, Electroseismic investigation of the shallow subsurface: Field measurements and numerical modeling: Geophysics, **62**, 97–105.

Millar, J., 1995, A source of life made commercial: Phyics World, **8**, no. 10, 22–23.

Pride, S. R., and Haartsen, M. W., 1996, Electroseismic wave properties: J. Acoust. Soc. Am., **100**, 1301–1315.

Pride, S. R., and Morgan, F. D., 1991, Electrokinetic dissipation induced by seismic waves: Geophysics, **56**, 914–925.

Pride, S. R., 1994, Governing equations for the coupled electromagnetics and acoustics of porous media: Phys. Rev. B., **50**, 15678–15696.

Revil, A., Pezard, P. A., and Glover, P. W. J., 1999, Streaming potential in porous media: 1. Theory of the zeta potential: J. Geophys. Res., **104**, 20021–20031.

Russell, R. D., Butler, K. E., Kepic, A. W., and Maxwell, M., 1997, Seismoelectric exploration: The Leading Edge, **16**, 1611–1615.

Thompson, A., and Gist, G., 1993, Geophysical applications of electrokinetic conversion: The Leading Edge, **12**, 1169–1173.

Zhu, Z., Haartsen, M. W., and Toksöz, M. N., 1999, Experimental studies of electrokinetic conversions in fluid-saturated borehole models: Geophysics, **64**, 1349–1356.